Heat-Induced Gelation of β-Lactoglobulin. 1. Time-Resolved Dynamic Light Scattering

Shin-ich Takata, Tomohisa Norisuye, Naoki Tanaka, and Mitsuhiro Shibayama*

Department of Polymer Science and Engineering, Kyoto Institute of Technology, Matsugasaki, Sakyo-ku, Kyoto 606-8585, Japan

Received February 23, 2000; Revised Manuscript Received May 16, 2000

ABSTRACT: The time evolution of the dynamics of globular protein during the gelation process via aggregation has been studied by time-resolved dynamic light scattering (DLS) for β-lactoglobulin (β-LG) in aqueous solutions at pH 2 and 7. The following facts were disclosed: (1) The scattered intensity, $\langle I\rangle_T$, started to fluctuate, and the intensity−time correlation function (ITCF) exhibited a power-law behavior ($g^{(2)}(\tau) - 1 \sim \tau^{\alpha-1}$) at the gelation threshold, t_{th}. (2) The variations of $\langle I\rangle_T$'s were different between the two pHs, a gradual increase for pH 2 and a stepwise increase followed by a plateau for pH 7. (3) The exponent α was found to be strongly dependent on pH. The values of α were 0.51 ± 0.05 for pH 2 and 0.74 ± 0.05 for pH 7. (4) A strong concentration and pH dependence of t_{th} was also observed in both cases. These findings indicate that β-LG gels formed at pH 2 and pH 7 have different architectures, i.e., loosely tied networks (for pH 2) and fractal aggregates (for pH 7) of protein molecules.

Introduction

Globular proteins undergo thermal denaturation. There exist many types of denatured states including several types of intermediates, which result in aggregation and gelation. It is well-known that the kinetics of aggregate formation and the structure of aggregates are strongly dependent on its environmental condition, such as pH, temperature, and ionic strength. Among a large number of globular proteins, β-lactoglobulin (β-LG) is one of the most extensively studied globular proteins on thermal aggregation.[1−7] Griffin et al. studied heat-induced aggregation of β-LG in solution in order to understand the molecular details of protein aggregation, i.e., the physics of protein association and the process of gel formation.[8] β-LG contains two disulfide groups and one cysteine sulfydryl group per monomer. In general, it is believed that aggregation is governed by a delicate balance among hydrophobic interaction, hydrogen bonding, disulfide bonding, electrostatic interactions, and so on. A transparent gel of β-LG can be obtained at pH 2 and low ionic strength, whereas the gel becomes opalescent at pH 7 and high ionic strength.[9] The mechanism of aggregation, however, has not been fully elucidated. Gimel et al. reported that β-LG aggregates formed at pH 7 with 0.1 M added salt have a self-similar structure ranging over a few tens to hundreds of nanometers.[5] Aymard et al. showed by scattering experiments and size exclusion chromatography that the aggregation of β-LG at pH 7 consists of a two-step mechanism: formation of (1) small globular aggregates by interchange of disulfide bonds and (2) bigger aggregates by physical interactions.[10] They also studied differences in the structure of aggregates formed at pH 2 and 7 by light and small-angle neutron scattering[11] and reported that β-LG undergoes aggregation in the presence of 0.1 M salt with fractal dimensions of 2.0 (for pH 7) and 1.8 (for pH 2). According to the work, the persistence length increases by lowering the concentration of the added salt. They concluded that the structure of aggregates is strongly dependent on both pH and ionic concentrations. Recently, they reported that the ionic strength is a determining factor of the structure.[12] However, these studies were mainly conducted on samples thermally quenched from a reactor batch in which aggregation took place at an elevated temperature. Therefore, the structure might be subject to change during the course of quenching.

Recently, we developed an in-situ time-resolved dynamic light scattering (TRDLS) method for analyses of a gelation process of polymeric systems. The TRDLS allows one to determine gelation threshold by four characteristic features: (i) an abrupt increase in the scattered intensity, (ii) a power law behavior in the intensity−time correlation function (ITCF), (iii) a characteristic broadening of the decay time distribution function, and (iv) a suppression of the initial amplitude in ITCF.[13,14] Here, we apply this technique to investigate the aggregation and gelation process of β-LG. First of all, the pH dependence of the cluster distribution of β-LG molecules in an aqueous solution at room temperature is discussed, which is followed by the kinetics of heat-induced gelation of β-LG in both acidic and neutral conditions. Then, the physical meaning of the power-law exponent is discussed.

Theoretical Section

The intensity−time correlation function (ITCF), $g^{(2)}(\tau)$, is given by

$$g^{(2)}(\tau) \equiv g^{(2)}(\tau;q) = \frac{\langle I(0;q)\, I(\tau;q)\rangle_T}{\langle I(0;q)\rangle_T^{\,2}} = |g^{(1)}(\tau;q)|^2 + 1 \quad (1)$$

where $I(\tau;q)$ is the scattered intensity at time τ with respect to $\tau = 0$ and the scattering vector q, and $\langle\cdots\rangle_T$ denotes time average. $g^{(1)}(\tau)$ is the scattering field time-correlation function given by

$$g^{(1)}(\tau) = \int_0^\infty G(\Gamma) \exp(-\Gamma\tau)\, d\Gamma \quad (2)$$

$G(\Gamma)$ is the characteristic decay time distribution func-

* To whom correspondence should be addressed.

10.1021/ma0003295 CCC: $19.00
Published on Web 07/06/2000

tion, where Γ^{-1} is the characteristic decay time. For a monodisperse system, $G(\Gamma) = \delta(\Gamma - \Gamma_0)$. Hence,

$$g^{(1)}(\tau) = \exp(-\Gamma_0\tau) \quad \text{(monodisperse)} \tag{3}$$

where Γ_0 is the characteristic decay rate for a monodisperse system. In general, however, $G(\Gamma)$ is evaluated from $g^{(1)}(\tau)$ with an inverse Laplace transform. For a narrow-disperse system, the apparent hydrodynamic radius, $R_{H,app}$, can be estimated by

$$R_{H,app} = \frac{kTq^2}{6\pi\eta\langle\Gamma\rangle} \tag{4}$$

where k is the Boltzmann constant, T is the absolute temperature, η is the solvent viscosity, and $\langle\Gamma\rangle$ is the average of the characteristic decay rate, i.e.,

$$\langle\Gamma\rangle \equiv \frac{\int_0^\infty G(\Gamma)\Gamma\, d\Gamma}{\int G(\Gamma)\, d\Gamma} \tag{5}$$

When a gelling system approaches the gelation threshold, i.e., $t \approx t_{th}$, $g^{(1)}(\tau)$ cannot be expressed by eq 3 and $g^{(1)}(\tau)$ is accompanied by either a stretched exponential function or a power-law function. Hence, the intensity−time correlation function (ITCF) is then given by[15]

$$g^{(2)}(\tau) - 1 = \sigma_I^2\{A\exp(-\Gamma_f\tau) + (1 - A)\exp[-(\Gamma_s\tau)^\beta]\}^2 \quad (t < t_{th}) \tag{6}$$

or

$$g^{(2)}(\tau) - 1 = \sigma_I^2\{A\exp(-\Gamma_f\tau) + (1 - A)[1 + (\tau/\tau^*)]^{(\alpha-1)/2}\}^2 \quad (t \approx t_{th}) \tag{7}$$

where Γ_f, Γ_s, and τ^* are characteristic decay rates for the fast mode and the slow mode and the lower cutoff of the slow mode (i.e., a power-law behavior), respectively. A ($0 < A < 1$) is the fraction of the fast mode (collective diffusion). α is the fractal dimension of the scattered photons introduced by Martin et al.[16] for the power-law behavior in DLS. σ_I^2 is the initial amplitude of $g^{(2)}(\tau) - 1$, and $\sigma_I^2 \approx 1$ and $\sigma_I^2 \ll 1$ for ergodic and nonergodic media, respectively. For $\tau \gg \tau^*$, eq 7 becomes a power law function at the gelation threshold, i.e.,

$$g^{(2)}(\tau) - 1 \sim \tau^{\alpha-1} \quad (\text{for } \tau \gg \tau^* \text{ and } t \approx t_{th}) \tag{8}$$

A power-law behavior in ITCF has been indeed observed by many workers.[15−19] The value of α reported in the literature is in the range 0.2−0.73.

On the other hand, it is also well-known that gelation threshold can be detected by a rheological measurement. Winter et al. showed that the storage $G'(\omega)$ and loss moduli $G''(\omega)$ exhibit a power-law behavior with angular frequency, ω, i.e.,[20,21]

$$G' = G'' \sim \omega^n \quad \text{(at the gelation threshold)} \tag{9}$$

where n is the viscoelastic exponent. The physical meaning of n is extensively discussed by Muthukumar.[22,23] The value of n is dependent on the degree of hydrodynamic screening and of the excluded-volume interaction. There are several arguments on the relationship between the viscoelastic exponent n and the DLS exponent α. According to Martin et al.,[16] eq 9 leads to

$$G(\tau) \sim \tau^{-d\nu/(d\nu+k)} \tag{10}$$

and

$$g^{(2)}(\tau) - 1 \sim \tau^{-2\beta/(\nu+k)} \tag{11}$$

where d is the space dimension; ν, β, and k are the exponents related to the correlation length, the gel fraction, and the viscosity, respectively. Fang obtained these exponents for the case of poly(methyl methacrylate) cross-linked by ethylene dimethacrylate; $\beta = 0.39$, $\nu = 0.89$, and $k = 1.33$.[24] By substituting $d = 3$ to eq 11, one obtains $G(\tau) \sim \tau^{-0.667}$ and $g^{(2)}(\tau) - 1 \sim \tau^{-0.351}$. These experimental values support the relationship $n \approx \alpha$ obtained by Adam and Lairez although the relation was derived erroneously.[25] Doi and Onuki, on the other hand, showed a different relationship from arguments on the dynamic coupling between stress and composition of polymeric media,[26]

$$G(t) \sim \tau^{-n}, \quad g^{(2)}(\tau) - 1 \sim \tau^{-2n} \tag{12}$$

This leads to

$$n = (1 - \alpha)/2 \tag{13}$$

Though the discussion by Doi and Onuki seems to be robust, their theoretical prediction does not account for the experimental results, i.e., $n \approx \alpha$. Therefore, the physical meaning of α obtained by DLS has not been clarified yet. Having this fact in mind, we discuss the DLS exponent α for β-LG aggregates prepared at different pHs.

Experimental Section

1. Samples. β-Lactoglobulin (β-LG), crystallized for three times followed by lyophilized, was purchased from Sigma (lot no. 114H7055) which is known to be a mixture of variants A and B. The molecular weight is 18 400. Aqueous solutions of β-LG were prepared by dissolving β-LG in distilled water. The concentrations were C = 0.02, 0.05, and 0.10 g/mL. Each solution was filtered with a 0.20 μm filter. The pH of the solutions was adjusted by adding NaOH or HCl aqueous solutions. After filtration, the protein concentrations were determined by UV spectrometry using an extinction coefficient of 0.961/cm g^{-1}.[27]

2. **Time-Resolved Dynamic Light Scattering (TRDLS).** TRDLS measurements were carried out on an ALV compact goniometer system, ALV, Langen, Germany, coupled with a 22 mW helium−neon laser source. Intensity−time correlation functions (ITCF) were collected with the sampling time of 60 s without time interval throughout aggregation process for about 5 h at 75 °C. This allowed us an in-situ monitoring of the variation in both the scattered intensity, $I(t;q)$, and ITCF during the course of aggregation time t. It should be noted that, despite the employment of such a low power laser, a high level of photon signals over 50 times larger in intensity than a conventional system comprising a set of pinholes and a photomultiplier was acquired owing to an avalanche photodiode and static−dynamic enhancer. The scattering angle, θ, was varied from 30° to 150° for q-dependent experiments, while a fixed angle, i.e., 90°, was chosen for time-resolved light scattering measurements.

Results and Discussion

1. pH Dependence of β-LG Aqueous Solutions. Figure 1 shows a series of decay time distribution

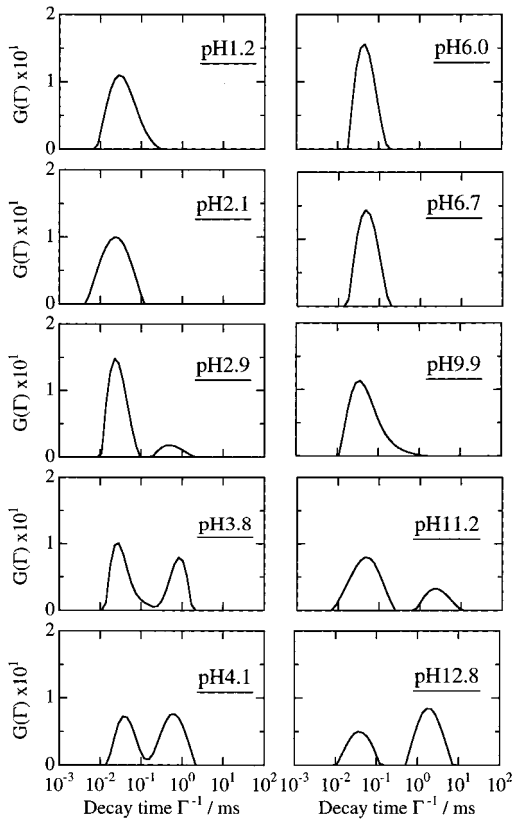

Figure 1. pH dependence of the decay time distribution function, $G(\Gamma)$, for β-LG aqueous solutions ($C = 0.0176$ g/mL).

functions, $G(\Gamma)$, obtained for β-LG aqueous solutions at different pHs. The scattering angle was 90°. The concentration was fixed to be $C = 0.0176$ g/mL (the nominal value being 0.02 g/mL). For pH ≤ 2.1, $G(\Gamma)$ has a single peak. According to eq 4, $R_{H,app}$ was estimated to be about 2 nm at pH 2. In the range of pH 2.9 and 4.1, however, there appeared double peaks, which are assigned to β-LG monomers (more rigorously a mixture of monomers and dimers) for the fast mode and their aggregates for the slow mode. The size of the aggregates is estimated to be in the range 30−150 nm by employing eq 4. In the region between pH 6.0 and 9.9, a single peak is recovered in $G(\Gamma)$. Double peaks appeared again for pH > 11.2. Figure 1 shows that β-LG does not aggregate owing to isoelectric balance at room temperature both at around pH 2 and pH 7. Hence, we chose β-LG aqueous solutions at pH 2 and 7 for studies of heat-induced aggregation (i.e., gelation).

Figure 2 shows the pH dependence of $R_{H,app}$ for $C = 0.0176$ g/mL. In the pH region indicated by the shade (around the isoelectric point,[1] pH 5.2), a phase separation takes place. Below this pH, β-LG molecules prefer a molecular dispersion, while the dimer form is preferable at higher pHs according to the literature.[2] Pessen et al. observed proton relaxation rates of water in dilute solutions of β-LG by NMR and obtained a similar phase diagram.[2] The monomer−dimer transition of β-LG was extensively studied by Aymard.[28] They reported that not only pH but also monomer and salt concentrations and temperature also affect the monomer−dimer transition. The strong pH sensitivity is ascribed to the capability of hydrogen bond of the β-sheet structure of the strand I (the 140th−150th residues).[3] It should also be noted that β-LG is remarkably acid stable, resisting denaturation and remaining intact at pH 2.[3] However, we

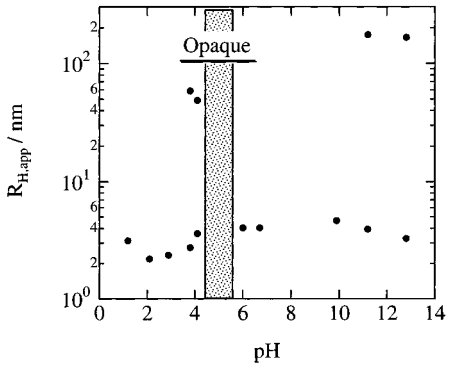

Figure 2. Variation of the apparent hydrodynamic radius, $R_{H,app}$, of β-LG in aqueous solutions ($C = 0.0176$ g/mL). The shaded part indicates the region where the solution became opaque.

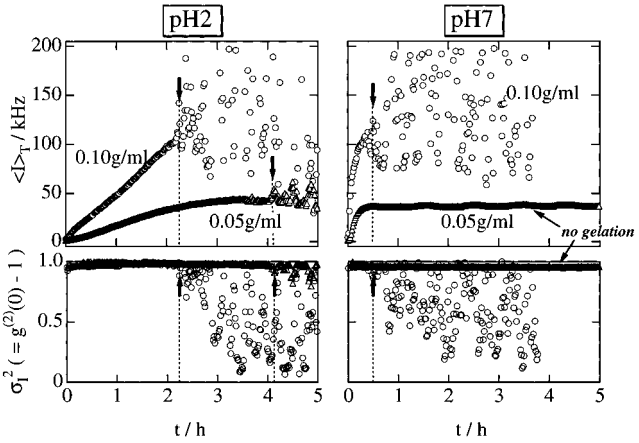

Figure 3. Time evolution of the scattered intensity $\langle I\rangle_T$ (upper) and the initial amplitude of ITCF, σ_I^2 (lower), during heat-induced denaturation process of β-LG at 75 °C for pH 2 (left) and 7 (right). The arrows indicate the time at gelation threshold, t_{th}.

conclude that a larger scale aggregation or a phase separation undergoes exclusively in this pH region since the system becomes opaque.

2. Aggregation and Gelation Kinetics. Heat-induced aggregation (denaturation) takes place at an elevated temperature. The denaturation temperature, T_d, is reported to be ca. 67 °C for β-LG at pH 7 by differential calorimetry.[29] Griffins et al. observed an increase of the mean hydrodynamic diameter for β-LG at pH 7 by heat treatment above 70 °C.[8] On the other hand, Griko and Privalov reported $T_d \approx 78$ °C for β-LG at pH 2.[4] These reports indicate that β-LG at pH 2 is more thermoresistant than at pH 7. By knowing this fact, we carried out a time-resolved dynamic light scattering for β-LG aqueous solutions both at pH 2 and 7 by temperature jump to 75 °C ($> T_d$). These pHs were chosen since the system in the initial stage did not contain aggregates and pH dependence of gelation process can be studied without disturbance of aggregates.

Figure 3 shows the time variations of the scattered intensity $\langle I\rangle_T$ and the initial amplitude of ITCF, $\sigma_I^2 \equiv g^{(2)}(\tau=0) - 1$, for β-LG aqueous solutions at (a) pH 2 and (b) pH 7 after temperature jump to 75 °C. Two concentrations were chosen here to examine effects of protein concentration on gelation. In the case of pH 2, $\langle I\rangle_T$ started to fluctuate at $t = 2.12$ and 4.14 h respectively for $C = 0.10$ and 0.05 g/mL. These times are

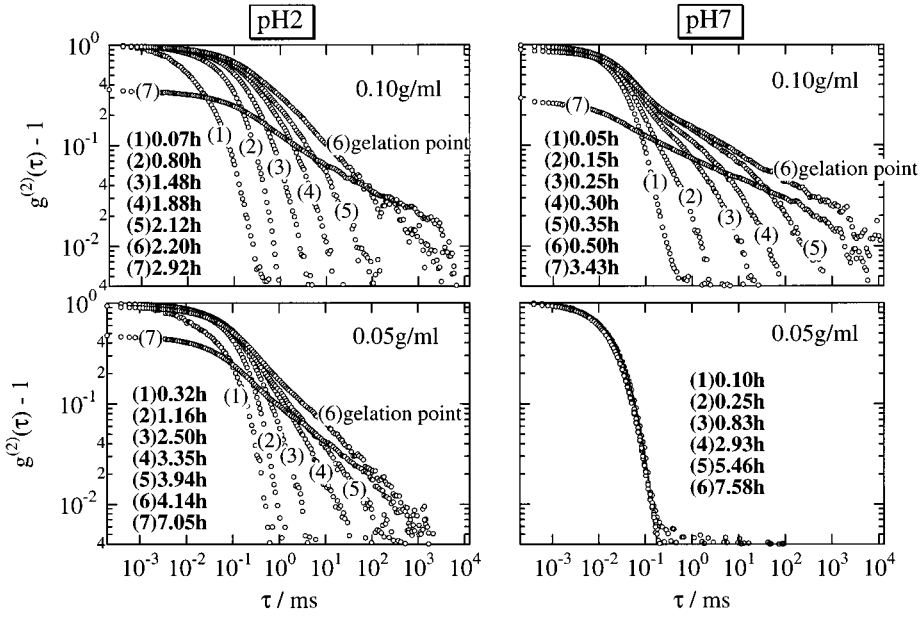

Figure 4. Changes of ITCFs of β-LG during heat-induced denaturation process at 75 °C for pH 2 (left) and 7 (right). Note that no specific change occurs for β-LG with 0.05 g/mL and pH 7 (right bottom).

assigned to be the time at gelation threshold, t_{th}, since the onset of gelation can be detected by an abrupt increase and appearance of strong fluctuations in $\langle I \rangle_T$ and depression of σ_I^2 from unity.[14] Note here that a macroscopic gelation threshold was also determined by examining flow behavior for a reference sample during the same gelation process and was found to be roughly identical to that obtained by DLS. Such an agreement in the gelation time between the macroscopic and the microscopic (DLS) gelation threshold was obtained in other systems, e.g., in tetramethoxysilane (TMOS) gels[30] and in thermoreversible physical gels of the poly(vinyl alcohol)−Congo Red complex.[31] Although only a very small scattering volume, e.g., 0.1 mm^3, is examined for the determination of gelation threshold, the TRDLS method demonstrates to be sensitive enough for determination of gelation threshold. It should be also noted here that the abrupt intensity rise does not mean phase separation. The system was transparent, and no phase separation was detected at all throughout the gelation process at both pH 2 and 7.

When pH was raised to 7, gelation was fastened to 0.50 h for $C = 0.10$ g/mL. When the concentration was reduced to 0.05 g/mL, however, no gelation took place at pH 7 as indicated by no characteristic change in $\langle I \rangle_T$ and σ_I^2. In this case, no macroscopic gel formation was observed at all even though the heat treatment time was prolonged to 3 days. This experimental result indicates that the concentration dependence is stronger in the case of pH 7 than of pH 2. A gelation was also observed at $C = 0.08$ g/mL. Hence, the lowest concentration for gelation is deduced to be 0.05 g/mL $< C <$ 0.08 g/mL at pH 7. It should be noted here this criterion is also dependent on the ionic strength.

Another interesting feature is the variation of $\langle I \rangle_T$ with t. In the case of β-LG at pH 2, a time-linear function was observed for $\langle I \rangle_T$ with t, while $\langle I \rangle_T$ for pH 7 exhibits a rapid increase at the very beginning of aggregation followed by a gradual increase (i.e., a convex-upward type function) as shown in Figure 3. A similar behavior was also observed in TMOS gels. That is, the variation of $\langle I \rangle_T$ with t depends on the choice of catalyst, i.e., a gradual increase in $\langle I \rangle_T$ for the case of acid catalyst and a convex-upward type increase for the case of basic catalyst.[30] Hence, an analogy between the two systems is found in the variation of $\langle I \rangle_T$. This strong pH dependence of gelation kinetics may be ascribed to difference in the architecture of clusters as will be discussed later. It is noteworthy that the convex-upward type function is an indication of reaction limited aggregation (RLA) process.[30,32,33] Rigorously speaking, the time variation of $\langle I \rangle_T$ for TMOS gels prepared by an acid catalyst did not follow a time-linear fashion but a rather a concave-upward function. However, this fact can be explained by a small deviation of the functionality from 2 (i.e., linear chain extension), such as 2.01, as discussed by Bechtold et al.[34]

In Figure 4, a series of ITCFs during polymerization process are displayed. As shown in the left-top figure, ITCF becomes broader with increasing polymerization time and finally exhibits a power law behavior, e.g., $t_{th} = 2.20$ h (curve 6) (for $C = 0.10$ g/mL at pH 2). Note the well-known fact that the ITCF obeys a power law at the gelation threshold.[14,16,17,19] After passing t_{th}, the ITCF becomes flattened (curve 7), and its initial amplitude, σ_I^2, deviates from unity as shown with an arrow in the left-bottom figure of Figure 3. Similar phenomena are also observed for the samples of $C = 0.05$ g/mL at pH 2 and 0.10 g/mL at pH 7. However, no changes in the ITCFs were observed for the pH 7 sample with 0.05 g/mL. This clearly indicates that 0.05 g/mL is too low to form infinite clusters at pH 7 although a rapid aggregation was also observed at pH 7. Instead, stable clusters of $R_{H,app} \approx 10$ nm are formed by heat. This result seems to agree well with the result reported by Aymard et al.[10] They carried out an in-situ small-angle neutron scattering experiment during aggregation process of a 4% β-LG solution in D_2O in the presence of 0.003 M and observed that the z-average radius of gyration increased rapidly in 5 h and finally reached a plateau value of 11.5 ± 0.5 nm.

3. Relationship between Cluster Structure and the Exponent. Figure 5 shows examples of curve fitting for the cases of $t = t_{th} = 2.21$ h at pH 2 and $t = t_{th} =$ 0.50 h at pH 7. As shown in this figure, the shapes of ITCFs are quite different between pH 2 and 7. The

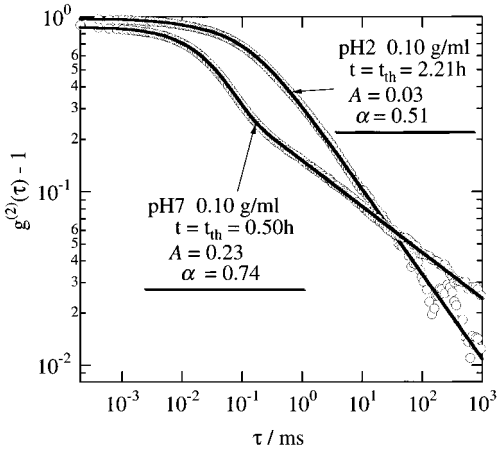

Figure 5. Power law analysis of ITCF at the gelation threshold, $t = t_{th}$, for TMOSs at pH 2 and pH 7.

contribution of the fast mode (diffusive mode) is much less for pH 2 ($A = 0.03$) compared to pH 7 ($A = 0.23$). This indicates that aggregates formed at pH 7 have a larger freedom of local motion (cooperative diffusion) compared with those prepared at pH 2. The value of the exponents were $\alpha = 0.51 \pm 0.05$ for pH 2, and the value of α remained constant irrespective of protein concentration in the range of $0.05 \leq C \leq 0.10$ g/mL. On the other hand, a different value $\alpha = 0.74 \pm 0.05$ was obtained for pH 7. The error here was determined by repeating the same experiment for several times with fresh samples.

The power-law behavior in ITCF has been observed by many workers. Adam et al. obtained $\alpha = 0.24-0.54$ for polyurethane clusters.[17] Martin et al. reported $\alpha = 0.73$ for silica gels prepared with a basic catalyst.[15,16] Lang and Burchard obtained $\alpha = 0.66$ for a thermoreversible gels of Tamarind Gum, i.e., a kernel polysaccharide, with solutions of Na_2SO_4.[18] Ren and Sorensen also obtained a power-law behavior in the ITCF for gelatin gels.[19] Recently we carried out a comparison of the structure for two types of silica gels prepared with an acid and base catalysts. The silica gels prepared with an acid catalyst exhibited $\alpha \approx 0.50$, while the gels prepared with a basic catalyst showed $\alpha \approx 0.73$. The following facts are known for silica gels by viscosity and small-angle X-ray scattering studies. Silica gels prepared with an acid catalyst consist of relatively long siloxane chains with occasional cross-linking, while those prepared with a basic catalyst have a high degree of branching.[35] An analogy seems to be present between the cases of silica gels and β-LG. In the case of β-LG aggregated at pH 2, the gel consists of relatively large polymer chains slightly connected to each other since the exponent ($\alpha = 0.51 \pm 0.05$) is quite close to that of silica gels ($\alpha \approx 0.56$) prepared with an acid catalyst. On the other hand, in analogy of the case of silica gels prepared with a base catalyst, $\alpha = 0.74 \pm 0.05$ obtained for pH 7 strongly suggests that the gel consists of fractal aggregates.

Figure 6 shows the q dependence of the exponent α for β-LG gels prepared at pH 2 and 7. The ITCFs were obtained for gels quenched at $t \approx t_{th}$ from 75 °C to room temperature. Since the apparent exponent deviates noticeably from α for $t < t_{th}$ or $t > t_{th}$, the values obtained for the quenched gels are somewhat different from the values obtained by TRDLS in Figure 5. However, Figure 6 indicates that the exponent α is

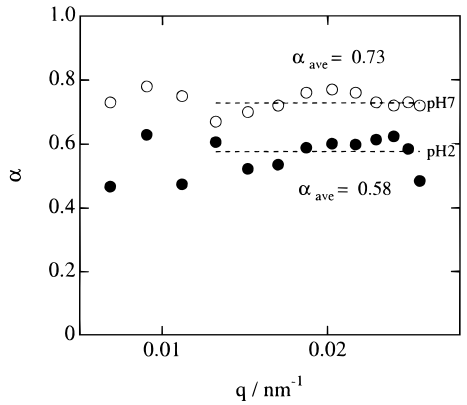

Figure 6. q dependence of the exponent, α, for β-LG gels near the gelation threshold. The dashed lines indicate the average obtained for $q \geq 0.0132$ nm^{-1} ($\theta \geq 60°$).

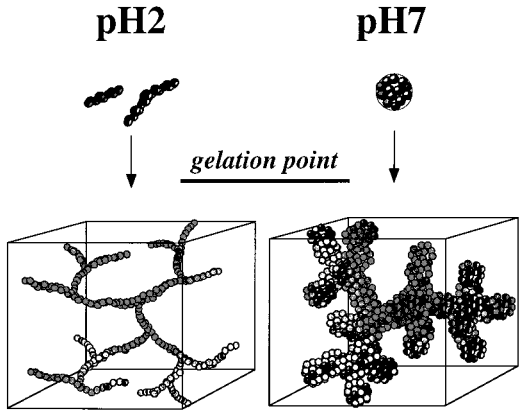

Figure 7. Schematic representation illustrating the structure of β-LG gels prepared at pH 2 and 7. At pH 2, β-LG monomers may be connected to form a chain during which cross-linking takes place occasionally. Hence, a network with low cross-link density is formed. On the other hand, β-LG at pH 7 has a strong tendency to stick each other, resulting in fractal aggregate formation.

independent of q at least in this q range ($60° \leq \theta \leq 150°$). Note that we ignored the first three data points ($30° \leq \theta \leq 50°$).

Figure 7 shows schematic illustrations of the network structures of β-LG prepared at pH 2 and 7. The TRDLS data strongly suggest that the gel network prepared at pH 2 consist of relatively long polypeptide chains with a few cross-links to each other. In this case, a polypeptide chain can propagate in the space, resulting in an effective formation of infinite clusters. On the other hand, at pH 7 β-LG forms fractal aggregates via reaction limited aggregation process, resulting in a higher value of α compared with the case of pH 2.

Conclusion

The time-resolved dynamic light scattering technique was applied to investigate heat-induced gelation kinetics of β-LG aqueous solution. The scattered intensity, $\langle I \rangle_T$, from β-LG aqueous solutions at 75 °C was monitored in-situ as a function of reaction time both at pH 2 and 7. $\langle I \rangle_T$ started to fluctuate at the gelation threshold, t_{th}. The variation of $\langle I \rangle_T$'s was different between the two pHs, i.e., a gradual increase for pH 2 and a stepwise increase followed by a plateau for pH 7. The intensity−time correlation function (ITCF) exhibited a power-law behavior ($g^{(2)}(\tau) - 1 \sim \tau^{\alpha-1}$) exclusively at t_{th}. The exponent α was found to be strongly dependent on pH.

The values of α were 0.51 ± 0.05 for pH 2 and 0.74 ± 0.05 for pH 7. These findings indicate that β-LG gels formed at pH 2 and pH 7 have different architectures, i.e., loosely tied networks (for pH 2) and fractal aggregates (for pH 7) of protein molecules.

Acknowledgment. This work is partially supported by the Ministry of Education, Science, Sports and Culture, Japan (Grant-in-Aid, 12450388 to M.S.). Thanks are due to the Cosmetology Research Foundation, Tokyo, for financial assistance.

References and Notes

(1) Kelly, M. J.; Reithel, F. J. *Biochemistry* **1971**, *10*, 2639.
(2) Pessen, H.; Purcell, J. M.; Farrell, H. M., Jr. *Biochim. Biophys. Acta* **1985**, *928*, 1.
(3) Papiz, M. Z.; Sawyer, L.; Eliopoulos, E. E.; North, A. C. T.; Findlay, J. B. C.; Sivaprasadarao, R.; Jones, T. A.; Newcomer, M. E.; Kraulis, P. J. *Nature* **1986**, *324*, 383.
(4) Griko, Y. V.; Privalov, P. L. *Biochemistry* **1992**, *31*, 8810.
(5) Gimel, J. C.; Durand, D.; Nicolai, T. *Macromolecules* **1994**, *25*, 583.
(6) Roefs, S. P. F. M.; de Kruif, K. G. *Eur. J. Biochem.* **1994**, *226*, 883.
(7) Dong, A.; Allison, S. D.; Chrisman, E.; Manning, M. C.; Carpenter, J. F. *Biochemistry* **1996**, *35*, 1450.
(8) Griffin, W. G.; Griffin, M. C. A.; Martin, S. R.; Price, J. *J. Chem. Soc., Faraday Trans.* **1993**, *89*, 3395.
(9) Kinsella, J. E.; Whitehead, D. M. *Adv. Food Nutr. Res.* **1989**, *31*, 343.
(10) Aymard, P.; Gimel, J. C.; Nicolai, T.; Durand, D. *J. Chim. Phys.* **1996**, *93*, 1996.
(11) Aymard, P.; Durand, D.; Nicolai, T. *Int. J. Polym. Anal. Charact.* **1996**, *2*, 115.
(12) Aymard, P.; Nicolai, T.; Durand, D.; Clark, A. *Macromolecules* **1999**, *32*, 2542.
(13) Norisuye, T.; Takeda, M.; Shibayama, M. *Macromolecules* **1998**, *31*, 5316.
(14) Norisuye, T.; Shibayama, M.; Tamaki, R.; Chujo, Y. *Macromolecules* **1999**, *32*, 1528.
(15) Martin, J. E.; Wilcoxon, J.; Odinek, J. *Phys. Rev. A* **1991**, *43*, 858.
(16) Martin, J. E.; Wilcoxon, J. *Phys. Rev. Lett.* **1988**, *61*, 373.
(17) Adam, M.; Delsanti, M.; Munch, J. P.; Durand, D. *Phys. Rev. Lett.* **1988**, *61*, 706.
(18) Lang, P.; Burchard, W. *Macromolecules* **1991**, *24*, 814.
(19) Ren, S. Z.; Shi, W. F.; Zhang, W. B.; Sorensen, C. M. *Phys. Rev. A* **1992**, *45*, 2416.
(20) Winter, H. H.; Chambon, F. *J. Rheol.* **1986**, *30*, 367.
(21) Winter, H. H.; Mours, M. *Adv. Polym. Sci.* **1997**, *134*, 167.
(22) Muthukumar, M.; Winter, H. H. *Macromolecules* **1986**, *19*, 1284.
(23) Muthukumar, M. *Macromolecules* **1989**, *22*, 4656.
(24) Fang, L. *Macromolecules* **1991**, *24*, 6839.
(25) Adam, M.; Lairez, D. In *Sol−Gel Transition*; Cohen Addad, J. P., Ed.; John Wiley & Sons: New York, 1996; p 87.
(26) Doi, M.; Onuki, A. *J. Phys. II* **1992**, *2*, 1631.
(27) Townend, R.; Weinberger, L.; Timasheff, S. N. *J. Am. Chem. Soc.* **1960**, *82*, 3175.
(28) Aymard, P.; Durand, D.; Nicolai, T. *Int. J. Biol. Macromol.* **1996**, *19*, 213.
(29) De Wit, J. N.; Swinkels, G. A. M. *Biochim. Biophys. Acta* **1980**, *624*, 40.
(30) Norisuye, T.; Inoue, M.; Shibayama, M.; Tamaki, R.; Chujo, Y. *Macromolecules* **2000**, *33*, 500.
(31) Ikkai, F.; Shibayama, M. *Phys. Rev. Lett.* **1999**, *82*, 4946.
(32) Martin, J. E. *Phys. Rev. A* **1987**, *36*, 3415.
(33) Lin, M. Y.; Lindsay, H. M.; Weitz, D. A.; Ball, R. C.; Klein, R.; Meakin, P. *Phys. Rev. A* **1990**, *41*, 2005.
(34) Bechtold, M. F.; Vest, R. D.; Plambeck, L. *J. Am. Chem. Soc.* **1968**, *90*, 4590.
(35) Brinker, C. J.; Scherer, G. W. *J. Non-Cryst. Solids* **1985**, *70*, 301.

MA0003295